

Esterification of Monochloroacetic Acid with *n*-Butanol Catalyzed by SBA-15 Supported Tungstophosphoric Acid

XUE JIANWEI and LIU CHUNLI*

Institute of Special Chemicals, Taiyuan University of Technology

Taiyuan, Shanxi 030024, P.R. China

E-mail: xuejianwei@yeah.net

The esterification reaction of monochloroacetic acid with *n*-butanol was carried out with heteropoly acid supported on SBA-15 as catalyst to replace mineral liquid acids. The experimental results indicated that heteropoly acid supported on SBA-15 had effective catalytic performance. The effects of various parameters such as mole ratio of acid to alcohol, reaction temperature, catalyst number and time of reaction were investigated. The optimum reaction conditions were as follows: molar ratio of alcohol to acid 1.3:1, temperature 130 °C, optimum loading amount 23 %, mass ratio of the catalyst used in the reactants 2.0 %, reaction time 5 h, esterification rate above 98 %. The activities of catalyst are stable after catalyst was reused 30 times.

Key Words: SBA-15, Heteropoly acid, Chloroacetate, Support, Esterification.

INTRODUCTION

n-Butyl-chloroacetate is an important organic intermediate, which is widely used in agricultural chemicals, medical chemicals, cosmetics, etc. In the traditional synthesis, the esterification reaction of monochloro-acetic acid with *n*-butanol is catalyzed using mineral liquid acids, such as sulphuric acid and *p*-toluene sulphonic acid. The catalytic activity of homogeneous catalysts is high. They suffer, however, from several drawbacks, such as their corrosive nature, the existence of side reactions and the fact that the catalyst cannot be easily separated from the reaction mixture¹⁻⁴. hence, some better catalysts are expected to be applied.

Heteropoly acid (HPA) catalysts have received considerable attention, because of their environmental compatibility, reusability, operational simplicity, greater selectivity, non-toxicity, non-corrosiveness and ease of isolation⁵. Being promising solid acids to replace environmentally harmful liquid acid catalysts, heteropolyacids are widely used in variety of acid catalyzed reactions such as esterification⁶, etherification⁷, hydration of olefin⁸, deesterification⁹, dehydration of alcohol¹⁰, polymerization of THF¹¹ and alkylation of phenol¹².

However, the main disadvantage is their very low surface area ($< 10 \text{ m}^2 \text{ g}^{-1}$), hence it becomes necessary to disperse heteropoly acid on supports that possess large surface area. SBA-15 is a newly discovered mesoporous silica molecular sieve with uniform tubular channels whose pore diameter is variable from 50 to 300 Å¹³. It has thicker pore wall and higher hydrothermal stability¹⁴, which would make it a suitable host for heteropoly acids. It is known that 12-tungstophosphoric acid ($\text{H}_3\text{PW}_{12}\text{O}_{40}$) is the strongest heteropoly acid in the Keggin series. The use of $\text{H}_3\text{PW}_{12}\text{O}_{40}$ supported on SBA-15 ($\text{H}_3\text{PW}_{12}\text{O}_{40}/\text{SBA-15}$) as solid catalysts for the esterification of chloroacetic acid with *n*-butanol was studied in this work.

EXPERIMENTAL

Catalyst preparation and characterization: 12-Tungstophosphoric acid supported on SBA-15 ($\text{H}_3\text{PW}_{12}\text{O}_{40}/\text{SBA-15}$) was prepared by reported method¹⁵. Samples were characterized by means of XRD patterns on a Rigaku D/max 2500 diffractometer instrument operating at 40 kV and 100 mA with Cu target $\text{K}\alpha$ -ray irradiation. N_2 adsorption-desorption measured at 77 K on a micromeritics NOVA 1200e volumetric system. FT-IR spectra measured using a BIO2RAD/FTS165 spectrometer at room temperature. Analyses performed using KBr pellet technique with a resolution at 2 cm^{-1} .

Synthesis of ester and analysis of esterification rate: Esterification reaction between monochloroacetic acid and alcohol was performed in a three-necked flask with a condenser at the reflux temperature. After the reaction, the catalysts were filtered, dried and reused. Analyses of the reaction products were performed by means of National Standards of People's Republic of China GB1668-95, GB-2895-82. The calculated equation of acid value X is $X = M \times 10^{-3} \times V \times C/G$, the unit of M is g/mol ; the V is volume of potassium hydroxide (unit is mL); the G is mass of ester. The C is concentration of potassium hydroxide (unit is mol/l). The calculated equation of esterification rate Y is $Y = (1-A/B) \times 100 \%$. The A is acid value before the reaction. The B is acid value after the reaction.

RESULTS AND DISCUSSION

The XRD patterns of pure SBA-15 and $\text{H}_3\text{PW}_{12}\text{O}_{40}/\text{SBA-15}$ are shown in Fig. 1. For all the samples the hexagonal structure of SBA-15 is confirmed by a typical XRD pattern consisting of a strong peak (at 2θ around 0.8°) along with two weak peaks (at 2θ around 1.6° and 1.8°)¹⁶. For the XRD pattern of $\text{H}_3\text{PW}_{12}\text{O}_{40}/\text{SBA-15}$, diffractions from (100) plane, (110) plane, (200) plane are shifted to larger 2θ angles, indicating the decrease in d -spacing. This is probably due to the restructuring during the step of absorption of $\text{H}_3\text{PW}_{12}\text{O}_{40}$ and the intensities of d_{100} , d_{110} and d_{200} are lower than those of pure SBA-15 because of the existence of $\text{H}_3\text{PW}_{12}\text{O}_{40}$. With

the increasing of the loading amount of $\text{H}_3\text{PW}_{12}\text{O}_{40}$, the diffractions appear as broad wide peaks, which indicating the losing of the long-range order.

According to the large angle XRD patterns ($2\theta = 5-40$), when the loading amount is smaller, no characteristic peaks of $\text{H}_3\text{PW}_{12}\text{O}_{40}$ are observed, indicating that $\text{H}_3\text{PW}_{12}\text{O}_{40}$ is probably finely dispersed on the surface of the sample or incorporated in the pore wall of the sample. However, with the increasing of the adding amount, the characteristic peaks were observed as shown in Figs. 4 and 5, indicating small quantity of crystallites of $\text{H}_3\text{PW}_{12}\text{O}_{40}$ existing on the surface.

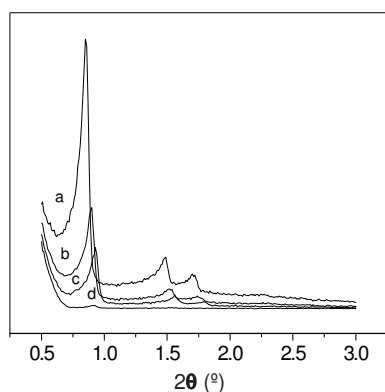


Fig. 1. XRD patterns of SBA-15 and $\text{H}_3\text{PW}_{12}\text{O}_{40}/\text{SBA-15}$ (a) SBA-15; (b) 28 % $\text{H}_3\text{PW}_{12}\text{O}_{40}/\text{SBA-15}$; (c) 33 % $\text{H}_3\text{PW}_{12}\text{O}_{40}/\text{SBA-15}$; (d) 38 % $\text{H}_3\text{PW}_{12}\text{O}_{40}/\text{SBA-15}$

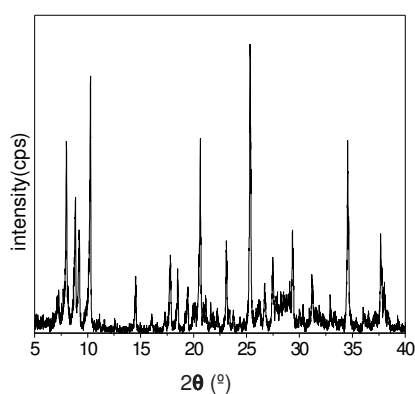


Fig. 2. XRD patterns of $\text{H}_3\text{PW}_{12}\text{O}_{40}\cdot x\text{H}_2\text{O}$

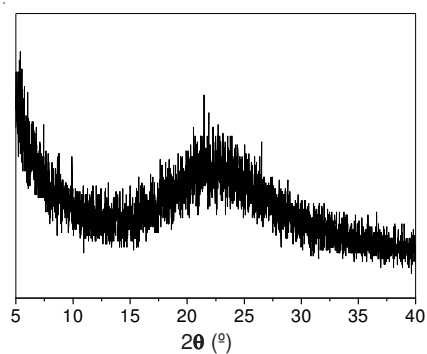


Fig. 3. XRD patterns of SBA-15

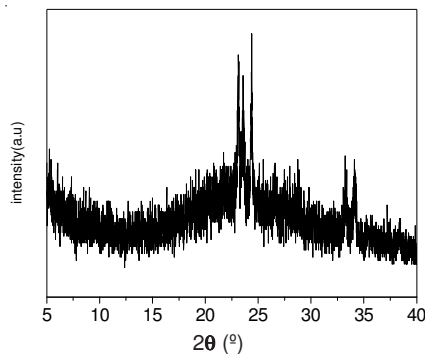


Fig. 4. XRD patterns of $\text{H}_3\text{PW}_{12}\text{O}_{40}/\text{SBA-15}$ (25 %)

Fig. 6 and Fig. 8 show the N₂ adsorption-desorption isotherms for pure SBA-15 and H₃PW₁₂O₄₀/SBA-15 respectively. Both the N₂ adsorption-desorption isotherms are the typical IV according to the IUPAC and exhibited an H1 hysteresis loop which is a characteristic of mesoporous solids¹⁷. From the curve, it is gained that BET surface area of SBA-15 is 1146.90 m² g⁻¹ and BET surface area of H₃PW₁₂O₄₀/SBA-15 is 742.88 m² g⁻¹. It is evident that the introduction of H₃PW₁₂O₄₀ decreases the surface-area and pore volume of pure SBA-15. It is explained that large quantity of H₃PW₁₂O₄₀ exists in the channel.

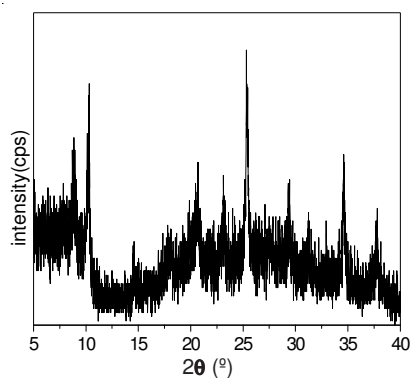


Fig. 5. XRD patterns of 43 % H₃PW₁₂O₄₀/SBA-15

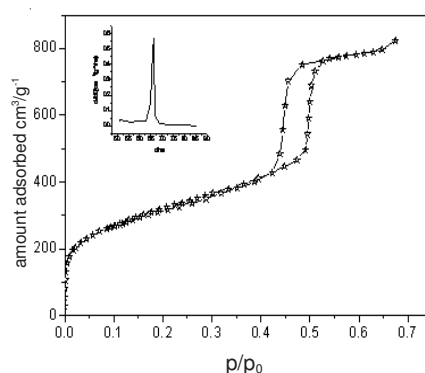


Fig. 6. N₂ Adsorption isotherm of SBA-15

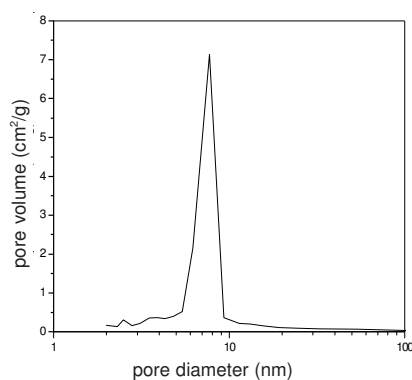


Fig. 7. Pore size distribution of H₃PW₁₂O₄₀/SBA-15 (20 %)

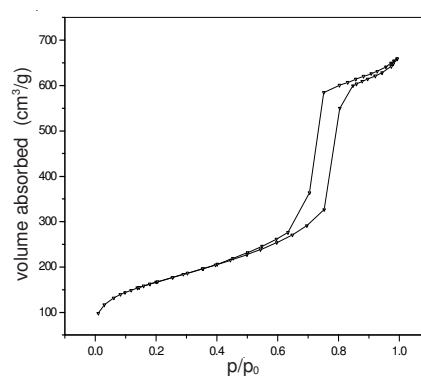


Fig. 8. N₂ Adsorption isotherms of H₃PW₁₂O₄₀/SBA-15 (20 %)

Effect of molar ratio of acid/alcohol on esterification: It is well known that the esterification reactions are reversible. Water, one of the products, must be removed in time, which is in favour of the reaction in present studies and we use cyclohexanone as water-carrying agent.

Esterification rate can be increased by increasing the concentration of either alcohol or acid. For economic reasons, the reactant that is usually the less expensive of the two is taken in excess. In present study, *n*-butanol was used in excess.

Fig. 9 shows that the esterification rate increases with the molar ratio up to 1.3:1. However, with the further increasing of the molar ratio, the relative concentration of the monochloroacetic acid will decrease, hence the esterification rate is lower.

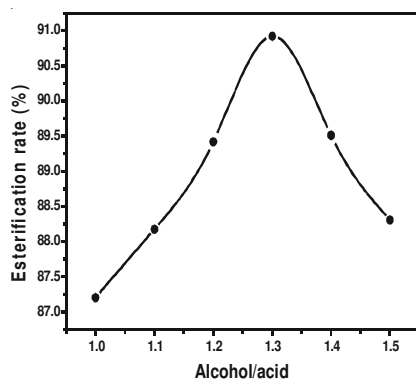


Fig. 9. Effect of molar ratio of alcohol/acid on esterification

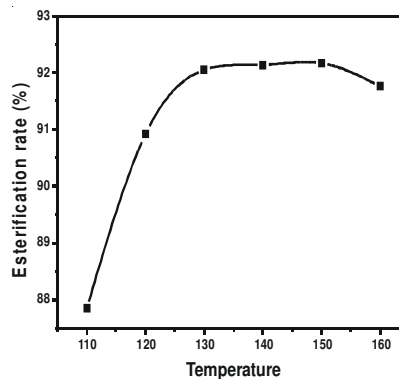


Fig. 10. Effect of temperature on esterification

Effect of temperature on esterification: Temperature is considered as an important factor to esterification rate. The increasing the temperature is apparently favourable for the acceleration of the forward reaction. In present studies, the esterification reaction was carried out at six different temperatures, The maximum esterification rate is reached at 150 °C. From Fig. 10, it is found that when the temperature reaches 130 °C, esterification rate reached to a high value. With the further increasing of the temperature, the esterification rate increases slowly, even to decrease. From economy, the optimum temperature is found to be 130 °C.

When the temperature surpassed 150 °C, the esterification rate reduced evidently, it is explained that high temperature can prompt the production of by-products.

Effect of loading amount of $H_3PW_{12}O_{40}$ on esterification: Fig. 11 shows the esterification rate is the highest when the loading amount is 23 %. While above 23 %, the esterification reactions were not distinctly enhanced. It is well-known that the more loadings, the smaller pore volume of the carrier is. The reactants are limited to enter into the pore of catalyst.

Effect of quantity of catalyst to esterification: Fig. 12 indicates that esterification rate increases along with the increasing amount of catalyst. After achieving the optimum value, esterification rate is not obviously raised. Therefore optimum catalyst amount is 2 wt.%.

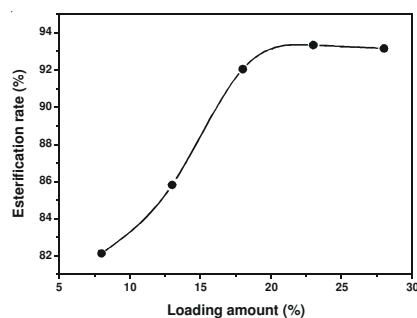


Fig. 11. Effect of loading amount of $H_3PW_{12}O_{40}$ on esterification

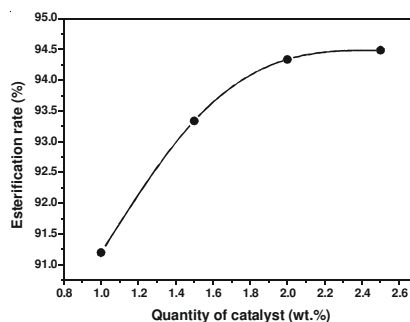


Fig. 12. Effect of quantity of catalyst on esterification

Effect of reaction time on esterification: Fig. 13 indicate that there is an increase in the esterification rate with the increase of reaction time, the best reaction time is found 5 h.

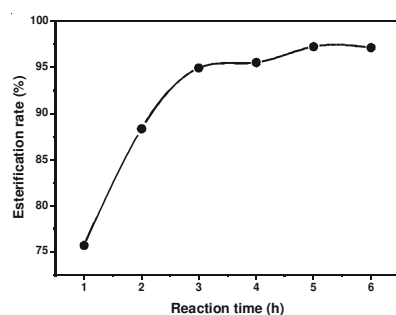


Fig. 13. Effect of reaction time on esterification

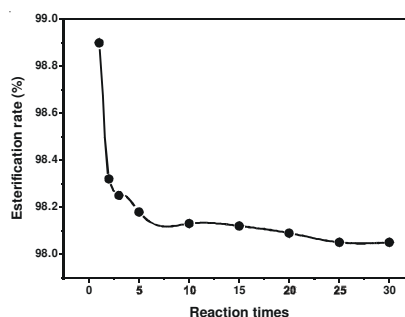


Fig. 14. The activity of catalyst

Reusability of catalyst: Fig. 14 shows that the esterification rate remained 98.05 % after repeated use of catalyst for 30 times. Verhoef *et al.*¹⁸ proposed that water (produced in the reaction) helps heteropoly acid migrate from the internal surface of the carriers to the outside surface, which causes the catalytic activity to reduce. In this experiment the catalyst were used for the second time, activity indeed dropped. After three times activity of catalyst maintained stable. It was possible that some $H_3PW_{12}O_{40}$ was absorbed on the outside of SBA-15. After several times of reaction, the absorbed $H_3PW_{12}O_{40}$ was dropped, hence the activity kept stable.

Conclusion

From the above data of the esterification rate, we can find that the 12-tungstophosphoric acid supported on the SBA-15($\text{H}_3\text{PW}_{12}\text{O}_{40}$ /SBA-15) is an excellent catalyst, the catalytic activity is high, the life length is long, the activity of catalyst isn't decreased after being reused for 30 times. The optimum reaction conditions were investigated as follows: molar ratio of alcohol /acid 1.3:1, temperature 130 °C, optimum loading amount 23 %, mass ratio of the catalyst used in the reactants 2.0 %, reaction time 5 h.

REFERENCES

1. M.R. Altiokka and A. Citak, *Appl. Catal. A: Gen.*, **239**, 141 (2003).
2. X. Chen, Z. Xu and T. Okuhara, *Appl. Catal. A: Gen.*, **180**, 261 (1999).
3. W.T. Liu and C.S. Tan, *Ind. Eng. Chem. Res.*, **40**, 3281 (2001).
4. G.D. Yadav and M.B. Thathagar, *React. Funct. Polym.*, **52**, 99 (2002).
5. A. Heydari, H. Hamadi and M. Pourayoubi, *Catal. Commun.*, **8**, 1224 (2007).
6. C. Hu, M. Hashimoto, T. Okuhara and M. Misono, *J. Catal.*, **143**, 437 (1993).
7. T. Okuhara, A. Kasai and M. Misono, *Shokubai (Catalyst)*, **22**, 226 (1980).
8. T. Yamada, *Petrotech (Tokyo)*, **13**, 627 (1990).
9. T. Okuhara, T. Nishimura, K. Ohashi and M. Misono, *Chem. Lett.*, 1201 (1990).
10. T. Okuhara, T. Nishimura, K. Ohashi and M. Misono, *Chem. Lett.*, 155 (1995).
11. A. Aoshima, S. Tonomura and S. Yamamatsu, *Adv. Technol.*, **2**, 127 (1990).
12. G.S. Kumar, M. Vishnuvarthan, M. Palanichamy and V. Murugesan, *J. Mol. Catal. A: Chem.*, **260**, 49 (2006).
13. D. Zhao, J. Feng, Q. Huo, N. Melosh, G.H. Fredrickson, B.F. Chmelka and G.D. Stucky, *Science*, **279**, 548 (1998).
14. X. Yuan, J. Shen and G. Li, *Chin. J. Catal.*, **23**, 9 (2002).
15. X.Z. Zhang, Y.H. Yue and Z. Gao, *Chem. J. Chin. Univ.*, **22**, 1169 (2001).
16. Z. Luan, M. Hartmann, D. Zhao and W. Zhou, *Chem. Mater.*, **11**, 1621 (1999).
17. M. Kruk, M. Jaroniec, C.H. Ko and R. Ryoo, *Chem. Mater.*, **12**, 1961 (2000).
18. M.J. Verhoef, P.J. Kooyman, J.A. Peters and H.V. Bekkum, *Microporous and Mesoporous Mater.*, **27**, 365 (1999).